

# High precision study of the $Q\bar{Q}$ potential from Wilson loops at large distances

Bram Bolder,<sup>1</sup> Thorsten Struckmann,<sup>2</sup> Gunnar S. Bali,<sup>3</sup> Norbert Eicker,<sup>1</sup> Thomas Lippert,<sup>1</sup> Boris Orth,<sup>1</sup> Klaus Schilling,<sup>1,2</sup> and Peer Ueberholz<sup>1</sup>

<sup>1</sup>*Fachbereich Physik, Bergische Universität, Gesamthochschule Wuppertal, Gaußstraße 20, 42097 Wuppertal, Germany*

<sup>2</sup>*NIC, Forschungszentrum Jülich, 52425 Jülich and DESY, 22603 Hamburg, Germany*

<sup>3</sup>*Department of Physics and Astronomy, The University of Glasgow, Glasgow G12 8QQ, Scotland*

(SESAM - T $\chi$ L Collaboration)

(Received 24 May 2000; revised manuscript received 13 July 2000; published 12 March 2001)

For lattice QCD with two sea quark flavors we study the static quark-antiquark potential  $V(R)$  in the regime where string breaking is expected. In order to increase the statistics, we make full use of the lattice information by including *all* lattice vectors  $\mathbf{R}$  to any given separation  $R=|\mathbf{R}|$  in the infrared regime. The corresponding paths between the lattice points are constructed by means of a generalized Bresenham algorithm as known from computer graphics. As a result, we achieve a determination of the Wilson loops in the range 0.8–1.5 fm with hitherto unknown precision. Finally, we discuss the impact of this approach on the signal of the transition matrix element between two- and four-quark states.

DOI: 10.1103/PhysRevD.63.074504

PACS number(s): 11.15.Ha, 12.38.Gc, 12.39.Mk, 12.39.Pn

## I. INTRODUCTION

Confinement of quarks is an issue of prime importance in the understanding of strong interaction physics. While the study of the static quark-antiquark potential from simulations of quantum chromodynamics has been pushed to rather high accuracy in quenched QCD and allows today for a precise determination of the string tension, the search for evidence of string breaking from Wilson loops in simulations of the full QCD vacuum has been futile so far. The linear rise of the static potential from Wilson loops seems to persist even in the presence of vacuum polarization by quark loops [1–6]. The common explanation for this finding is that the asymptotic time behavior of the Wilson loops cannot be resolved and that a multichannel analysis including light fermion operators is required to achieve sufficient ground state overlap in the available time range [7].

In fact, a fully fledged multichannel approach has been demonstrated to be a viable technique to realize breaking of the string between adjoint sources in pure gauge theories or fundamental color sources in Higgs models [8–10]. In the case of full QCD, however, it appears overly costly to achieve the required statistical accuracy of the generalized Wilson loops which incorporate light quark-antiquark pairs in the initial or final states [11]. The reason is that one is prevented from exploiting the translational symmetry, since this would require computation of light propagators  $P(y,x)$  on any source point location,  $x$  (see e.g. Refs. [11,12]). In Refs. [13,14] stochastic estimator methods with maximal variance reduction (so-called *all-to-all methods*) were applied to cope with the fluctuations on the multichannel correlator matrix, but failed so far to provide sufficient accuracy in the infrared regime.

On the other hand, if one scrutinizes existing QCD potential data from Wilson loops [1–6] for color screening one will notice that the statistical errors become substantial in the

region of interest,  $r \approx 1.2$  fm,<sup>1</sup> too. Thus, one might hope that QCD color screening could be detected with improved statistics on slightly extended time and space separations of Wilson loops.

The main purpose of the present paper is to improve on this point by pushing for a high precision “classical” Wilson loop calculation at large separations in  $N_f=2$  QCD. This is achieved by squeezing maximal information out of each vacuum configuration through rotational invariance and comprehensive utilization of *all possible R values* on the lattice. As a result of our “all- $R$  approach” (ARA) we are able to present a long range static potential from Wilson loops in unprecedented accuracy.

In Sec. II we shall describe how we go about in the buildup of nonplanar loops to any given  $\mathbf{R}$ . In Sec. III we apply the ARA both to standard Wilson loops and to the transition correlator between static and static-light quark states.

## II. LOOP CONSTRUCTION

Our aim is to increase statistics in the regime of color screening, i.e. for large quark-antiquark separations,  $R$ . Obviously, on such a length scale, a given QCD vacuum configuration contains plenty of information that can be exploited for self-averaging and thus for error reduction: first, one can realize, on a hypercubic lattice, a fairly dense set of  $R$  values; second, for a given large value of  $R=|\mathbf{R}|$ , there are many different three-vector realizations  $\mathbf{R}$  on the lattice.

We wish to make use of this fact by a systematic construction of off-axis Wilson loops,  $W(R,T)$ , in the range  $R_{\min} \leq R \leq R_{\max}$ , with  $R_{\min}=10 \approx 1.7R_0$  and  $R_{\max}=12\sqrt{3} \approx 3.5R_0$ , where  $R_0$  is the Sommer radius (in lattice units),

<sup>1</sup>We use uppercase (lowercase) letters for quantities in lattice units (physical units).

TABLE I. The number of different solutions to Eq. (1) obtained by the ARA for the interval  $10 \leq R \leq 12\sqrt{3}$ ,  $|R_i| \leq 12$ .

	No. $R$ values	No. $\mathbf{R}$ vectors	No. $\mathbf{R}$ vectors/ $R$ entry
Standard	21	302	14.4
ARA	175	11486	65.6

that amounts to  $r_0 \approx 0.5$  fm [15]. The construction proceeds by choosing all possible vectors,  $\mathbf{R}$ , with integer components  $C_{\min}, C_{\text{mid}}$ , and  $C_{\max}$  (in any order of appearance) that obey the inequalities

$$R_{\min}^2 \leq R^2 = C_{\min}^2 + C_{\text{mid}}^2 + C_{\max}^2 \leq R_{\max}^2, \quad (1)$$

where  $|C_{\min}| \leq |C_{\text{mid}}| \leq |C_{\max}|$ .

Subsequently, the set of solutions to the constraint, Eq. (1), is sorted according to the corresponding values of  $R$ . In Table I we display the large number of possible  $R$  values and vectors,  $\mathbf{R}$ , obtained in this way, with the additional restriction,  $|C_{\max}| \leq 12$ . So far, only  $\mathbf{R}$  vectors with  $(|C_{\max}|, |C_{\text{mid}}|, |C_{\min}|)$  being multiples of  $(1,0,0), (1,1,0), (1,1,1), (2,1,0), (2,1,1)$  or  $(2,2,1)$  have been considered [16–19]. Within the investigated regime,  $10 \leq R \leq 12\sqrt{3}$ , we achieve a gain factor of more than 8 in terms of the spatial resolution in  $R$  (from 21 to 175 different values). Moreover, the number of different  $\mathbf{R}$  vectors that yield the same distance,  $R$ , is increased by an average gain factor of more than 4. Accordingly, we find the ARA to reduce the statistical errors on potential values by factors of around 2.

We shall briefly discuss the construction of the gauge transporters connecting the quark and antiquark locations,  $\mathbf{R}_Q$  and  $\mathbf{R}_{\bar{Q}} = \mathbf{R}_Q + \mathbf{R}$ , which appear within the ARA nonplanar Wilson loops. In order to achieve a large overlap with the physical ground state we would like to construct lattice paths that follow as close as possible the straight line connecting  $\mathbf{R}_{\bar{Q}}$  with  $\mathbf{R}_Q$ . This task can be accomplished by a procedure which is known as the Bresenham algorithm [20] in computer graphics. There one wishes to map a straight continuous line between two points, say  $\mathbf{0}$  and  $\mathbf{C} = (C_{\max}, C_{\min})$ , onto discrete pixels on a 2D screen. Then one has to find the explicit sequence of pixel hoppings in the max and min directions such that the resulting pixel set mimics best the continuum geodesic between points  $\mathbf{0}$  and  $\mathbf{C}$ . The Bresenham prescription is simply to move in max direction unless a step in min direction brings you closer to the geodesic from  $\mathbf{0}$  to  $\mathbf{C}$ , where we assume  $|C_{\max}| \geq |C_{\min}|$ . It can easily be embod-

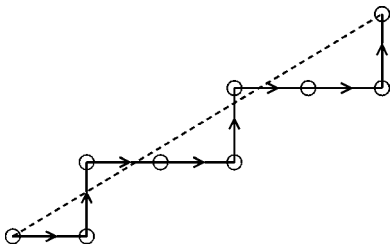


FIG. 1. Illustration of a path construction by the Bresenham algorithm, for  $\mathbf{C} = (5,3)$ .

ied into a fast algorithm based on local decision making only (see Fig. 1), by means of a characteristic lattice function  $\chi$  that incorporates the aspect ratio  $C_{\max}/C_{\min}$ .

The algorithm in two dimensions looks like

```
cmax 2: = 2 * cmax
```

```
cmin 2: = 2 * cmin
```

```
chi: = cmin 2 - cmax
```

```
FOR i: = 1 TO cmax DO
```

```
  step in max direction
```

```
  IF chi ≥ 0 THEN
```

```
    chi := chi - cmax 2
```

```
  step in min direction
```

```
  ENDIF
```

```
  chi := chi + cmin 2
```

```
ENDDO
```

The generalization to three dimensions is achieved by combining two of these 2D algorithms with different  $\chi$ 's for max-mid and max-min in just one loop over the max direction.

In order to convey an idea about the statistics gain inherent in such a systematic approach we have listed the number of  $\mathbf{R}$  vectors constructed in this manner in Table I. Note that for plane or space diagonal separations, we average over the two or six equivalent paths, respectively.

### III. THE STATIC POTENTIAL AT LARGE $R$

We base our analysis on 184 vacuum configurations, separated by one autocorrelation length, on  $L_\sigma^3 L_\tau = 24^3 \times 40$  lattices of  $N_f = 2$  QCD at  $\beta = 5.6$  and  $\kappa_{\text{sea}} = .1575$  [corresponding to  $m_\pi/m_\rho = .704(5)$ ], produced by the T $\chi$ L Collaboration on an APE 100 tower at INFN. These parameter values correspond to the biggest lattice volume at our disposal,  $L_\sigma a \approx 2$  fm. In order to minimize finite-size effects and possible violations of rotational symmetry on the  $L_\sigma = 24$  torus,  $C_{\max}$  has been restricted to  $|C_{\max}| \leq 12$ . The lattice constant  $a$  was determined from the Sommer radius  $r_0 = R_0 a \approx 0.5$  fm [15], as obtained in our previous investigation [19],  $R_0 = 5.89(3)$ .

#### A. Wilson loop operator

Before entering the Wilson loop analysis the configurations are smoothed by spatial APE or link smearing [21],

$$\text{link} \rightarrow \alpha \times \text{link} + \text{staples}, \quad (2)$$

followed by a projection back into the gauge group [16], with 26 such iterative replacements and the parameter value,  $\alpha = 2.3$ .

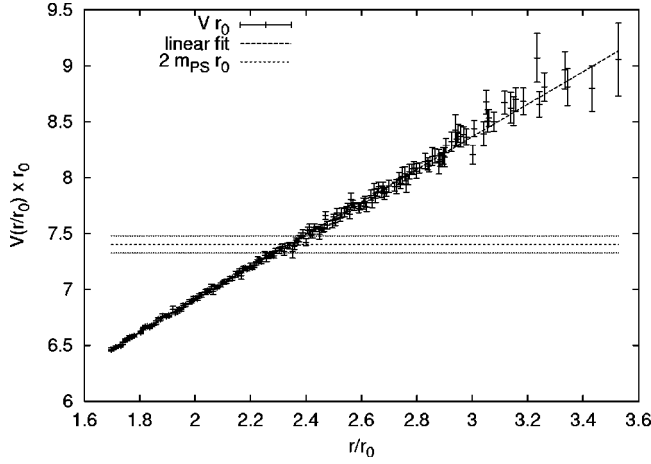


FIG. 2. The estimate on the static potential as obtained from Wilson loops at  $\kappa=0.1575$  and  $\beta=5.6$  on  $24^3 \times 40$  lattices, extracted from a single exponential fit to Wilson loops for  $4 \leq T \leq 8$ .

The potential values have been obtained by means of single and double exponential fits to smeared ARA Wilson loop data  $W(R, T)$  within the range,  $T_{\min} \leq T \leq 8$ . We shall quote statistical errors that are obtained by jackknifing. At the large  $R$  values that are of interest in view of screening effects, the quality of the statistical signal did not allow to include  $T$  values larger than 8.

In Fig. 2 we display estimates of the potential in the range  $1.7 \leq r/r_0 \leq 3.5$  obtained from a single exponential fit with  $T_{\min}=4$  (they agree with results from a double exponential fit with  $T_{\min}=1$ ). Note that for  $r > 2.4r_0$  the data are to be interpreted as strict upper limits on the potential. The slope is in agreement with the string tension,  $K = \sigma a^2 = 0.0372(8) = 1.139(4)R_0^{-2}$ , as quoted in Ref. [19] from a fit to data obtained at smaller  $r < 2.04r_0$ . Around the separation  $r_c \approx 2.3r_0$  the potential energy crosses the expected threshold for string breaking,  $2m_{PS}a = 1.256(13)$ , which is indicated by a horizontal error band. The errors quoted are statistical and are well below 1.5% for  $r/r_0 \leq 3$ . We find the data to follow perfectly a straight line: a flattening of the Wilson loop potential is not visible within the accessible  $T$  range and present statistical errors.

The quality of our data in the region up to  $T=8$  allows us to compute the overlaps with the ground and first excited states by means of two-exponential fits, as displayed in Fig. 3. Again our two data sets exhibit linear dependences on  $r$ , with nearly opposite slopes such that their sum turns out to be close to 1. The remainder does only slightly depend on  $r$  and is of order 10%.

### B. Transition operator

In a two-channel approach one extends the Wilson loop vacuum expectation value,  $C_{11}$ , to a  $2 \times 2$  correlation matrix  $C$  as pictogrammed in Fig. 4.

The quark propagators  $P(y, x)$  (wiggly lines) entering the remaining components of the correlation matrix  $C$  prevent the direct use of volume source averaging, which requires matrix inversions on *all* possible source points,  $x$ . Pennanen

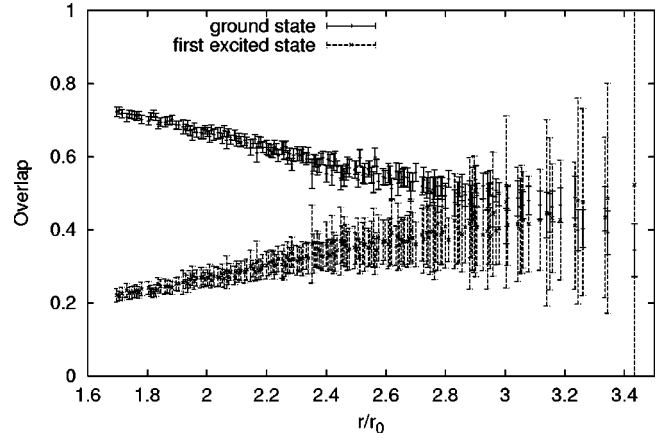


FIG. 3. The ground and first excited state overlaps (top and lower data sets, respectively) plotted versus the quark-antiquark separation, as obtained from Wilson loops. The data result from two-exponential fits in the region  $1 \leq T \leq 8$ .

and Michael have tested noisy estimator techniques on  $P$  for curing this problem but did not succeed in reaching the accuracy necessary to diagonalize  $C$  for  $r > r_c$  [14].

This motivates us to discuss the statistical quality of the transition matrix element  $C_{21}(R, T)$ , using only one light propagator and combinations of the ARA, spatial APE link smearing and source smearing techniques as known from spectrum calculations [22,23]. Here the smeared source is put to zero subsequently outside the volume  $|\mathbf{r}_s - \mathbf{x}| \leq R_q a$ , with  $R_q = 5$ .

While link smearing leaves us with errors of order 50% in the region  $R \leq 18$  at  $T=1$ , additional source smearing cuts down the noise amplitudes to a 20% level. Given the dense set of  $R$  values available from the ARA and in view of the fact that  $B(R) = \ln[C_{21}(R, T)]$  is a smooth function of  $R$ , there is opportunity to further improve by filtering the sequence,  $\{B(R)\} \rightarrow \{B_f(R)\}$ .

The idea is to trade in spatial resolution for the sake of error reduction. We apply a filter that consists of averaging over the data within a  $R_j$  window,  $|R_j - R| < R_f$ , with weights  $1/\sigma_j^2$ . The errors of the filter output are computed by the jackknife procedure. The effect of filtering is illustrated in Fig. 5 for  $R_f=0.5$  where we display the transition matrix element at  $T=5$  from the ARA (including link and source smearings)  $\{B(R)\}$  (upper sequence with large error bars) with the filtered one,  $\{B_f(R)\}$  (lower data sequence).

In order to display the systematics of windowing, we have refrained from thinning the latter sequence as one should in actual applications. We find a striking noise reduction

$$C = \begin{pmatrix} \square & \text{wiggly} \\ \text{wiggly} & \text{wiggly} - \text{wiggly} \end{pmatrix}$$

FIG. 4. The two channel correlation matrix  $C$ . Wiggly lines correspond to light quark propagators, solid lines to products of gauge links.

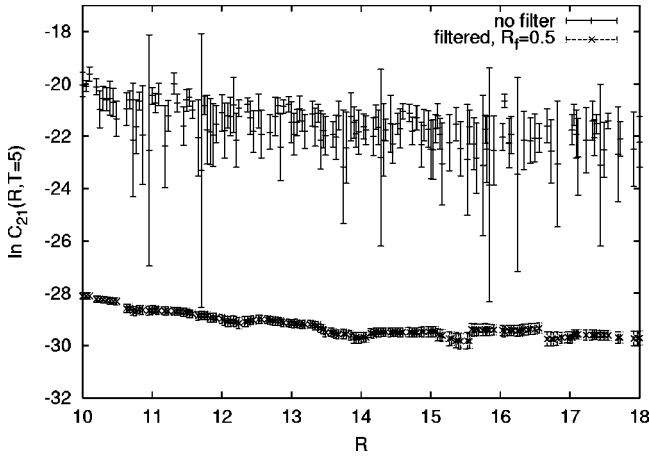


FIG. 5. The signal for  $\ln C_{21}$  at  $T=5$ . The filtered data have been vertically shifted by  $-8$  to avoid cluttering. String breaking is expected around  $R=13$ .

through filtering within the large distance regime,  $10 \leq R \leq 18$ : at  $T=3$  and  $T=5$  we encounter errors of less than 10% and 20%, respectively.

#### IV. SUMMARY AND CONCLUSIONS

Exploiting the dense set of  $R$  values available at large quark-antiquark separations on the lattice we succeeded in improving the precision of the  $Q\bar{Q}$  potential from Wilson loops in the string breaking regime by a factor of 2 with respect to standard methods. This enables us to analyze Wilson loop data well beyond the point where string breaking is

expected and corroborates previous conjectures that Wilson loops do not bear enough overlap with  $Q\bar{Q}q\bar{q}$  states for uncovering string breaking within the  $T$  range available at present.

The success of our all- $R$  approach to the Wilson loops in the string breaking regime has encouraged us to carry out a feasibility study on error control of the transition correlator,  $C_{21}$ . By additional use of source smearing and filtering techniques, we arrive at reasonable signal-to-noise ratios for  $\ln C_{21}$ .

For the final chord in a full two-channel analysis of  $Q\bar{Q}$  and  $Q\bar{Q}q\bar{q}$  states one would have to consider the correlator  $C_{22}$  which contains both a connected and a disconnected contribution: while the former might be tackled with our present techniques the latter might in our  $R$  range be dominated by  $\langle B \rangle \langle \bar{B} \rangle$  [24]. This is currently being investigated.

#### ACKNOWLEDGMENTS

We appreciate useful discussions with S. Güsken und M. Peardon during early stages of this research. K.S. thanks F. Niedermayer for an interesting discussion. This work was supported by DFG Graduiertenkolleg ‘‘Feldtheoretische und Numerische Methoden in der Statistischen und Elementarteilchenphysik.’’ G.B. acknowledges support from DFG grants Ba 1564/3-1, 1564/3-2 and 1564/3-3 as well as EU grant HPMF-CT-1999-00353. The HMC productions were run on an APE100 at INFN Roma. We are grateful to our colleagues F. Rapuano and G. Martinelli for the fruitful T $\chi$ L Collaboration. Analysis was performed on the Cray T3E system of ZAM at Research Center Jülich.

- 
- [1] HEMCGC Collaboration, U.M. Heller *et al.*, Phys. Lett. B **335**, 71 (1994).
  - [2] SESAM Collaboration, U. Glässner *et al.*, Phys. Lett. B **383**, 98 (1996).
  - [3] SESAM Collaboration, G.S. Bali *et al.*, Nucl. Phys. B (Proc. Suppl.) **63**, 209 (1998).
  - [4] CP-PACS Collaboration, S. Aoki *et al.*, Nucl. Phys. B (Proc. Suppl.) **73**, 216 (1999).
  - [5] UKQCD Collaboration, C.R. Allton *et al.*, Phys. Rev. D **60**, 034507 (1999); UKQCD Collaboration, J. Garden, Nucl. Phys. B (Proc. Suppl.) **83-84**, 165 (2000).
  - [6] MILC Collaboration, C. Bernard *et al.*, Phys. Rev. D **62**, 034503 (2000).
  - [7] S. Güsken, Nucl. Phys. B (Proc. Suppl.) **63**, 16 (1998).
  - [8] ALPHA Collaboration, F. Knechtli and R. Sommer, Phys. Lett. B **440**, 345 (1998).
  - [9] O. Philipsen and H. Wittig, Phys. Rev. Lett. **81**, 4056 (1998); **83**, 2684(E) (1999).
  - [10] P.W. Stephenson, Nucl. Phys. **B550**, 427 (1999).
  - [11] K. Schilling, Nucl. Phys. B (Proc. Suppl.) **83-84**, 140 (2000).
  - [12] G. S. Bali, Phys. Rep. **343**, 1 (2001).
  - [13] C. DeTar *et al.*, Nucl. Phys. B (Proc. Suppl.) **83-84**, 310 (2000).
  - [14] UKQCD Collaboration, P. Pennanen and C. Michael, hep-lat/0001015.
  - [15] R. Sommer, Nucl. Phys. **B411**, 839 (1994).
  - [16] G.S. Bali and K. Schilling, Phys. Rev. D **46**, 2636 (1992).
  - [17] G.S. Bali and K. Schilling, Phys. Rev. D **47**, 661 (1993).
  - [18] G.S. Bali, K. Schilling, and A. Wachter, Phys. Rev. D **56**, 2566 (1997).
  - [19] SESAM-T $\chi$ L Collaboration, G. Bali, B. Bolder, N. Eicker, Th. Lippert, B. Orth, P. Ueberholz, K. Schilling, and T. Struckmann, Phys. Rev. D **62**, 054503 (2000).
  - [20] See e.g., J. D. Foley *et al.*, *Computer Graphics: Principles and Practice* (Addison-Wesley, London, 1996).
  - [21] M. Albanese *et al.*, Phys. Lett. B **192**, 163 (1987).
  - [22] S. Güsken, Nucl. Phys. B (Proc. Suppl.) **17**, 361 (1990).
  - [23] SESAM Collaboration, N. Eicker *et al.*, Phys. Rev. D **59**, 014509 (1999).
  - [24] P. Pennanen *et al.*, Nucl. Phys. B (Proc. Suppl.) **83-84**, 200 (2000).